

New Mass Estimators For Tracer Populations

N.W. Evans, M.I. Wilkinson

Institute of Astronomy, Madingley Rd, Cambridge, CB3 0HA, UK

K.M. Perrett

Department of Physics, Queen's University, Kingston, Ontario, K7L 3N6, Canada

T.J. Bridges

Anglo-Australian Observatory, Epping, NSW, 1710 Australia

ABSTRACT

We introduce the *tracer mass estimator*. This is a new and simple way to estimate the enclosed mass from the projected positions and line of sight velocities of a tracer population (such as globular clusters, halo stars and planetary nebulae). Like the projected mass estimator, it works by averaging $(\text{projected distance}) \times (\text{radial velocity})^2 / G$ over the sample. However, it applies to the commonest case of all, when the tracer population does not follow the overall dark matter density. The method is verified against simulated datasets drawn from Monte Carlo realisations of exact solutions of the collisionless Boltzmann equation and applied to the recent M31 globular cluster data set of Perrett et al. (2002), as well as to M31's satellite galaxies.

Subject headings: galaxies: general – galaxies: haloes – galaxies: kinematics and dynamics – galaxies: individual: M31 – dark matter

1. Introduction

Simple estimators based on the virial theorem have long been used to ascertain the masses of galaxy groups from radial velocities and projected positions of the members (e.g. Zwicky 1933). Nowadays, they have been largely superseded by the projected mass estimator, which is based on averaging $(\text{projected distance}) \times (\text{radial velocity})^2 / G$ over the sample (Bahcall & Tremaine 1981; Heisler, Tremaine & Bahcall 1985). In the form in which it is usually encountered, a key assumption underlying the estimator is that the member galaxies track the mass of the group. The problem of estimating the masses of elliptical galaxies

and the haloes of spiral galaxies is different. Here, the datasets available are the radial velocities and projected positions of tracer populations, such as dwarf galaxy satellites, globular clusters, distant halo stars and planetary nebulae or PNe (see e.g., Wilkinson et al. 2002 for a recent review). These do not follow the underlying mass distribution which is dominated by the dark matter. For nearby galaxies, the advent of wide-field imaging and efficient planetary nebulae spectrographs (e.g., Méndez et al. 2001; Halliday et al. 2002) means that the quality and quantity of such datasets are destined to improve dramatically in the next few years.

The purpose of this paper is to present a new and simple mass estimator for galaxy haloes tailored for tracer populations and to apply them to new datasets for the Andromeda (M31) galaxy. It is the generalisation of the projected mass estimator to the commonest case of all – namely that when the number density of the tracer population is different from the overall mass density.

2. Simple Mass Estimators

On dimensional grounds, any mass estimator derived from projected data on a set of N tracer objects involves weighted means of $v_{\text{los}i}^2 R_i / G$, where $v_{\text{los}i}$ is the line of sight velocity (relative to the mean or systemic velocity) and R_i the projected position of the i th object relative to the center of the galaxy. The projected mass estimator is

$$M = \frac{C_{\text{proj}}}{GN} \sum_i v_{\text{los}i}^2 R_i. \quad (1)$$

This was introduced by Bahcall & Tremaine (1981) for test particles orbiting point masses (such as stars around a black hole or distant companion galaxies orbiting a central massive galaxy). The constant $C_{\text{proj}} = 16/\pi$ for test particles with an isotropic velocity distribution orbiting a point mass, whereas $C_{\text{proj}} = 32/\pi$ for test particles moving on radial orbits. Subsequently, Heisler et al. (1985) extended the projected mass estimator to the case in which the galaxy members are believed to track the total mass, such as galaxy groups. The constant $C_{\text{proj}} = 32/\pi$ for particles with an isotropic velocity distribution, whereas $C_{\text{proj}} = 64/\pi$ for particles moving on radial orbits.

We wish to generalise the mass estimator (1) to the case when the objects are drawn from a tracer population (such as globular clusters or PNe) between radii r_{in} and r_{out} . Let us assume that the tracer population is spherically symmetric and has a number density which falls off like a power-law

$$\rho(r) = \rho_0 \left(\frac{a}{r} \right)^\gamma, \quad r_{\text{in}} \lesssim r \lesssim r_{\text{out}}, \quad (2)$$

within the region of interest. The underlying gravity field is assumed to be scale-free

$$\psi(r) = \begin{cases} \frac{v_0^2}{\alpha} \left(\frac{a}{r}\right)^\alpha & \text{if } \alpha \neq 0, \\ -v_0^2 \log r & \text{if } \alpha = 0. \end{cases} \quad (3)$$

When $\alpha = 1$, this corresponds to test particles orbiting a point-mass; when $\alpha = 0$, the satellites are moving in a large-scale mass distribution with a flat rotation curve; when $\alpha = \gamma - 2$, the satellites follow the total self-gravitating mass (the case studied by Heisler et al. 1985). Properties of such tracer populations in scale-free spherical potentials have been deduced by Evans, Häfner & de Zeeuw (1997).

Suppose our tracers are distributed over a range of projected radii R_{in} and R_{out} (corresponding to the three-dimensional radii r_{in} and r_{out}). What mass distribution do they probe? By Newton’s theorem, there is no knowledge whatsoever on the mass distribution outside r_{out} . Accordingly, the best we can do is to estimate the total mass within the radius of the most distant satellite, namely

$$M = \frac{v_0^2 a^\alpha}{G} r_{\text{out}}^{1-\alpha}, \quad (4)$$

from the dataset of positions and velocities. Let (r, θ, ϕ) be standard spherical polars with the z axis defining the line of sight, so that the projected position R is $r \sin \theta$. Denoting the phase space distribution function of the tracer population by f , then the average value of $v_{\text{los}}^2 R$ in the survey is

$$\langle v_{\text{los}}^2 R \rangle = \frac{1}{M_t} \int \int f v_{\text{los}}^2 R d\mathbf{v} dr = \frac{4\pi}{M_t} \int_{r_{\text{in}}}^{r_{\text{out}}} dr \int_0^{\pi/2} d\theta \rho \sigma_{\text{los}}^2 r^3 \sin^2 \theta. \quad (5)$$

Here, we have computed the average over the ensemble between the radii r_{in} and r_{out} probed by our data. In this formula, σ_{los} is the line of sight velocity dispersion, while M_t is the mass in the tracer population, which is given by

$$M_t = \begin{cases} \frac{4\pi a^\gamma \rho_0}{3-\gamma} [r_{\text{out}}^{3-\gamma} - r_{\text{in}}^{3-\gamma}] & \text{if } \gamma \neq 3, \\ 4\pi a^3 \rho_0 \log(r_{\text{out}}/r_{\text{in}}) & \text{if } \gamma = 3. \end{cases} \quad (6)$$

2.1. Isotropic Populations

For the moment, let us assume that the velocity distribution of the tracers is isotropic so that the radial velocity dispersion σ_r is the same as the tangential σ_t . In this case, Evans

et al. (1997) solve the Jeans equations and derive the result

$$\rho\sigma_{\text{los}}^2 = \rho\sigma_r^2 = \frac{\rho_0 v_0^2}{\alpha + \gamma} \left(\frac{a}{r}\right)^{\alpha+\gamma}. \quad (7)$$

For example, if the potential is isothermal ($\alpha = 0$) with a flat rotation curve of amplitude v_0 and the density of the population falls off like $r^{-\gamma}$, then the velocity dispersion is just $v_0/\sqrt{\gamma}$ – which is a well-known result from the last century (e.g., Smart 1938). Now, substituting (6) and (7) into (5), we obtain:

$$\langle v_{\text{los}}^2 R \rangle = \frac{\pi^2 \rho_0 v_0^2}{M_t(\alpha + \gamma)} \int_{r_{\text{in}}}^{r_{\text{out}}} dr r^3 \left(\frac{a}{r}\right)^{\alpha+\gamma} = \frac{GM\pi}{4(\alpha + \gamma)} \frac{3 - \gamma}{4 - \alpha - \gamma} \frac{1 - (r_{\text{in}}/r_{\text{out}})^{4 - \alpha - \gamma}}{1 - (r_{\text{in}}/r_{\text{out}})^{3 - \gamma}}. \quad (8)$$

In other words, suppose we gather positions and velocities for a population of globular clusters or PNe with a three-dimensional number density falling like $r^{-\gamma}$ between an inner radius r_{in} and an outer radius r_{out} . The mass enclosed within the outermost datapoint is given by the simple formula

$$M = \frac{C}{GN} \sum_i v_{\text{los}_i}^2 R_i, \quad (9)$$

with

$$C = \frac{4(\alpha + \gamma)}{\pi} \frac{4 - \alpha - \gamma}{3 - \gamma} \frac{1 - (r_{\text{in}}/r_{\text{out}})^{3 - \gamma}}{1 - (r_{\text{in}}/r_{\text{out}})^{4 - \alpha - \gamma}}. \quad (10)$$

We refer to this as *the tracer mass estimator*. At first sight, it seems that the constant C in eq (10) is singular when the tracer population density falls off like r^{-3} (that is, $\gamma = 3$) or when $\alpha + \gamma = 4$ (for example, if the tracer population density falls off like r^{-4} in an isothermal ($\alpha = 0$) potential). However, a careful application of L'Hôpital's rule shows that the constants are well-defined. They are listed in Table 1 for convenience.

How do we set the parameters occurring in eq (10)? It is always reasonable to assume that $r_{\text{in}} \approx R_{\text{in}}$, where R_{in} is the projected radius of the innermost datapoint. If the dataset is derived from a wide-angle survey, in which the population is traced out to large radii, then it is also reasonable to assume that $r_{\text{out}} \approx R_{\text{out}}$, the projected radius of the outermost datapoint. But, this assumption is not appropriate for a dataset restricted to the inner parts only, because this will usually contain objects at larger three-dimensional radii projected into the sample. The parameter γ can be calculated from the surface density of the tracer population between R_{in} and R_{out} . However, α (and also possibly r_{out}) need to be set using astrophysical considerations. We are envisaging applications to the outer parts of galaxies probed by globular clusters and PNe, and so it is reasonable to set $\alpha \approx 0$ as the potential is probably close to isothermal. For example, Wilkinson & Evans (1999) studied the Milky Way galaxy and found that a near-isothermal potential is valid out to ~ 170 kpc.

Table 1: The constant C in the tracer mass estimator eq (9) for the two special cases ($\gamma = 3$ and $\alpha + \gamma = 4$). The number densities of tracer populations belonging to the spheroid or stellar halo are often $\propto r^{-3}$ or $\propto r^{-4}$ in the outer reaches, so the special cases often occur in practice.

Case	Constant
$\gamma = 3$	$C = \frac{4(\alpha+3)(1-\alpha)}{\pi} \frac{\log(r_{\text{out}}/r_{\text{in}})}{1-(r_{\text{in}}/r_{\text{out}})^{1-\alpha}}$
$\alpha + \gamma = 4$	$C = \frac{16}{\pi(3-\gamma)} \frac{1 - (r_{\text{in}}/r_{\text{out}})^{3-\gamma}}{\log(r_{\text{out}}/r_{\text{in}})}$

Comparison of the result (9-10) with previous work is instructive. For example, when $\alpha = 1$, the potential is Keplerian and we find that

$$M = \frac{4(1+\gamma)}{\pi GN} \sum_i v_{\text{los}i}^2 R_i. \quad (11)$$

When $\alpha = \gamma - 2$, the tracer population follows the underlying dark matter density and we find that

$$M = \frac{16(\gamma-1)}{\pi GN} \frac{1}{[1+(r_{\text{in}}/r_{\text{out}})^{3-\gamma}]} \sum_i v_{\text{los}i}^2 R_i. \quad (12)$$

These are not quite the same as the results given by Bahcall & Tremaine (1981) and Heisler et al. (1985). These investigators assumed that the sample was gathered from the center of the galaxy or cluster to infinity. In a number of integration by parts, boundary terms could therefore be legitimately dropped under the assumption $r^3 \rho \sigma_r^2 \rightarrow 0$ as $r \rightarrow 0$ and as $r \rightarrow \infty$. In our calculation, we have always performed the averaging over a finite range of radii and the contribution from the boundaries does not generally vanish. This is the origin of the difference. Even when we formally take the limit $r_{\text{in}} \rightarrow 0$ and $r_{\text{out}} \rightarrow \infty$, the boundary terms still do not vanish as the density distribution (2) of the tracer population is cusped. Of course, such a limit is purely formal, as our estimator is derived under the assumption that the power-law density distribution holds over a certain régime only.

2.2. Anisotropic Populations

Now let us extend the calculation to deal with populations with anisotropic velocity distributions, although still retaining the assumption of spherical symmetry for the density

distribution. Binney’s (1981) anisotropy parameter $\beta = 1 - \sigma_t^2/\sigma_r^2$ is often used to measure the relative importance of the radial σ_r and tangential σ_t velocity dispersions. When $\beta \rightarrow -\infty$, this is the circular orbit model and when $\beta = 1$, this is the radial orbit model. For models in which the anisotropy β does not vary with radius, the line of sight velocity dispersion σ_{los} is related to the radial velocity dispersion by

$$\sigma_{\text{los}}^2 = \sigma_r^2(1 - \beta \sin^2 \theta). \quad (13)$$

Substituting into (5), we find

$$\langle v_{\text{los}}^2 R \rangle = \frac{\pi^2(4-3\beta)}{4M_t} \int_{r_{\text{in}}}^{r_{\text{out}}} \rho \sigma_r^2 r^3 dr. \quad (14)$$

The radial velocity dispersion σ_r of the tracer population is (Evans et al. 1997)

$$\rho \sigma_r^2 = \frac{\rho_0 v_0^2}{\alpha + \gamma - 2\beta} \left(\frac{a}{r}\right)^{\alpha + \gamma}. \quad (15)$$

From this, we deduce

$$M = \frac{C}{GN} \sum_i v_{\text{los}_i}^2 R_i, \quad (16)$$

with

$$C = \frac{16(\alpha + \gamma - 2\beta)}{\pi(4-3\beta)} \frac{4 - \alpha - \gamma}{3 - \gamma} \frac{1 - (r_{\text{in}}/r_{\text{out}})^{3-\gamma}}{1 - (r_{\text{in}}/r_{\text{out}})^{4-\alpha-\gamma}} \quad (17)$$

This is the extension of the result to populations with constant anisotropy. Unless there are compelling reasons to the contrary (e.g., a highly flattened system supported by an anisotropic velocity dispersion), we advocate assuming isotropy. The value of eq (16) is that it enables us to calculate the error in making such an approximation. For example, suppose we consider tracer populations with a number density falling like r^{-4} in an isothermal potential. The anisotropy of stellar populations is not usually more extreme than 2 : 1. Therefore, eq (16) tells us that mistakenly assuming isotropy leads to mass underestimates (overestimates) in the case of radial (tangential) anisotropy of $\sim 30\%$.

2.3. Monte Carlo Simulations

We test the performance of the mass estimator with Monte Carlo realisations of exact solutions of the collisionless Boltzmann equation. The phase space distribution functions corresponding to power-law density profiles in power-law potentials are given in Evans et al.

Table 2: The percentage of mass estimates in error by a large factor (too big or too small by 50 per cent). The numbers are derived from 10000 Monte Carlo simulations of isotropic tracer populations with a number density falling like r^{-4} in an isothermal potential. The sample size N and extent $r_{\text{out}}/r_{\text{in}}$ are chosen so as to be typical of datasets of satellite galaxies (upper panel) and globular clusters (lower panel).

Estimator	Number	$r_{\text{out}}/r_{\text{in}}$	Too Low	Too High
Tracer	10	100	20%	37%
Projected	10	100	53%	11%
Virial	10	100	87%	0%
Tracer	100	10	2%	2%
Projected	100	10	72%	0%
Virial	100	10	100%	0%

(1997). To generate Monte Carlo realisations, the speed is picked from the distributions

$$f(v) \propto \begin{cases} v^{2-2\beta} \left| \psi(r) - \frac{1}{2}v^2 \right|^{[2\gamma-3\alpha-2\beta(2-\alpha)]/(2\alpha)} & \text{if } \alpha \neq 0, \\ v^{2-2\beta} \exp\left(-\frac{v^2}{2\sigma^2}\right) & \text{if } \alpha = 0. \end{cases} \quad (18)$$

For $\alpha > 0$, the maximum velocity at any position is $\sqrt{2\psi(r)}$; for $\alpha \leq 0$, the velocities can become arbitrarily large. Following Binney & Tremaine (1987), let us introduce spherical polar coordinates in velocity space (v, ξ, η) , so that the velocities resolved in spherical polar coordinates with respect to the center are then

$$v_r = v \cos \eta, \quad v_\theta = v \sin \eta \cos \xi, \quad v_\phi = v \sin \eta \sin \xi. \quad (19)$$

If ξ is generated uniformly in $[0, 2\pi]$, while η is picked in $[0, \pi]$ from the distribution

$$F(\eta) \propto |\sin \eta|^{1+2\beta} \quad (20)$$

then the velocities are generated with the correct anisotropy. Finally, a random projection direction is chosen and the line of sight velocity v_{los} and projected position R calculated. This gives us synthetic datasets of anisotropic spherical tracer populations in spherical haloes with which to test the performance of our mass estimators.

Figure 1 shows the medians and quartiles for the mass estimates of 10000 samples constructed from Monte Carlo realisations. We test the tracer mass estimator for both

isotropic (eq. 9) and anisotropic (eq. 16) populations, as well as the projected and virial mass estimators in the forms

$$M_{\text{proj}} = \frac{32}{\pi GN} \sum_i v_{\text{los}_i}^2 R_i, \quad M_{\text{virial}} = \frac{3\pi N}{2G} \frac{\sum_i v_{\text{los}_i}^2}{\sum_i 1/R_i}. \quad (21)$$

For each of the mass estimators, four models are shown in each panel. In the upper two panels, the tracer population has a number density falling like r^{-4} and is generated between R_{in} and $R_{\text{out}} = 10R_{\text{in}}$, while the rotation curve is flat ($\alpha = 0$), The models vary in the anisotropy of the velocity distribution (either $\sigma_t : \sigma_r = 1 : 1$ or $\sigma_t : \sigma_r = 2 : 1$ or $\sigma_t : \sigma_r = 1 : 2$). In upper panel, the number of objects is $N = 10$, which is typical for a sample of satellite galaxies. In the middle panel, the number of objects is $N = 100$, which is realistic for a sample of globular clusters with radial velocities. Finally, in the lower panel, the rotation curve is falling in a “half-way Keplerian” manner ($\alpha = 1/2$) and the tracer population is falling like r^{-3} . The sample size is again $N = 10$. The tracer mass estimator outperforms the projected and virial mass estimators in every case. This is as it should be, since the tracer mass estimator has been devised for the precise purpose of mass estimation from tracer populations, while the other two estimators have been devised with other applications in mind. It is interesting to ask how often the estimates are too low or too high by 50%. This information is recorded in Table 2 for some of the simulations. The projected and virial mass estimators yield systematic underestimates if they are mistakenly applied to tracer populations. Further, the situation is not improved by increasing the size of the tracer population – the estimators merely converge to an underestimated mass.

Finally, we test the tracer mass estimator against synthetic datasets drawn from a self-consistent Plummer model with a core radius b . This is a important thing to do as the tracer estimator has been derived for, and tested against, the scale-free case. The Plummer model is only approximately scale-free well outside the core region ($r \gg b$). The potential, density and distribution of speeds are

$$\rho \propto \frac{1}{(r^2 + b^2)^{5/2}}, \quad \psi \propto \frac{1}{(r^2 + b^2)^{1/2}}, \quad f(v) \propto v^2(\psi(r) - \frac{1}{2}v^2)^{7/2}. \quad (22)$$

Figure 2 shows how the estimators fare for sample sizes $N = 10$ and $N = 100$ using datasets gathered in the outer parts ($R_{\text{in}} = 10b, R_{\text{out}} = 100b$) and including some core contamination ($R_{\text{in}} = b, R_{\text{out}} = 100b$). For a self-consistent population, the projected mass estimator performs well, as it should do. Nonetheless, the tracer mass estimator (with $\gamma = 5, \alpha = 1$ and $\beta = 0$) gives slightly better results. The reason why the tracer mass estimator still out-performs the projected mass estimator is that the former includes a correction for the limited radial coverage of the sample, whereas the latter does not.

3. Application: the Andromeda Galaxy

It is important to know the mass of the Andromeda Galaxy (M31) for a number of reasons. First, the density profiles of dark matter haloes are an important constraint on cosmological theories of galaxy formation (e.g., Sellwood 2001). The haloes of nearby galaxies are particularly important as they can be studied in much greater detail. Second, the current generation of pixel lensing experiments towards M31 (e.g., Aurière et al. 2001, Paulin-Henriksson et al. 2002) requires an accurate estimate of the total mass so as to constrain the fraction in compact objects capable of producing microlensing events. We shall consider two datasets which probe Andromeda’s dark halo, namely the globular clusters and the dwarf spheroidal satellite galaxies.

3.1. Globular Clusters

Perrett et al. (2002) give the positions, velocities and metallicities for over 200 globular clusters in M31 out to a projected distance ~ 30 kpc. The data were obtained using fiber optic spectroscopy on the *William Herschel Telescope* and the typical errors on the radial velocities are ± 12 km s $^{-1}$. When combined with earlier data from Huchra, Brodie & Kent (1991), this gives a grand total of ~ 300 globular clusters. From the bimodality of the metallicity distribution, Perrett et al. show that the M31 globular clusters fall into metal-poor and metal-rich categories with different kinematics. As judged from the double Gaussian fit to the metallicity distribution, there are 177 globular clusters with a probability of belonging to the halo of greater than 90%. The cumulative number distribution of the halo globular clusters is shown in Figure 3. Only beyond 30 arcmin does the projected number density of the halo globulars fall off like a power-law, namely R^{-3} . Accordingly, we work with the 89 halo globular clusters with projected radii greater than 30 arcmin. The mean rotation amplitude of this sub-sample is $\langle v_\phi \rangle \approx 110$ km s $^{-1}$. Adopting a distance of 770 kpc, the globular clusters lie in projection between 6.8 kpc and 33 kpc. However, the globular cluster population in M31 certainly extends out to ~ 100 kpc (e.g., Hodge 1992). Using Monte Carlo simulations to build samples of 88 globular clusters with $6.8 \text{ kpc} < R < 33 \text{ kpc}$, we find that typically 20% of the sample have $r > 33$ kpc with the outermost datapoints typically at $r \approx 100$ kpc. Accordingly, in the formula for the tracer mass estimator, we set $\alpha = 0$ (isothermal-like galaxy), $\gamma \approx 4$, $r_{\text{in}} = 6.8$ kpc and $r_{\text{out}} \approx 100$ kpc.

The Jeans equation for a population with constant anisotropy β about a mean velocity $\langle v_\phi \rangle$ is (e.g., Binney & Tremaine 1987, section 4.2)

$$\frac{GM(r)}{r} = \langle v_\phi \rangle^2 - \sigma_r^2 \left[\frac{\partial \log \rho \sigma_r^2}{\partial \log r} + 2\beta \right] \quad (23)$$

The first term on the right-hand side describes the contribution of rotation to $M(r)$, the second term the contribution of pressure. With obvious notation, we write

$$\frac{GM_{\text{rot}}}{r} = \langle v_\phi \rangle^2, \quad \frac{GM_{\text{press}}}{r} = -\sigma_r^2 \left[\frac{\partial \log \rho \sigma_r^2}{\partial \log r} + 2\beta \right] \quad (24)$$

We compute $M_{\text{rot}} \sim 3 \times 10^{11} M_\odot$ directly from the mean rotation amplitude of the sample. We use the tracer mass estimator, applied to the observational data with the mean rotation velocity subtracted from the line of sight velocity, to compute $M_{\text{press}} \sim 9 \times 10^{11} M_\odot$ assuming isotropy. Hence, the total mass within ~ 100 kpc of the center of M31 is $\sim 1.2 \times 10^{12} M_\odot$. Note the tracer mass estimator applies to a pressure-supported tracer population and therefore any net rotation of the system must be subtracted before the velocities are used to estimate M_{press} .

How does the result from the tracer mass estimator compare with earlier work? Evans & Wilkinson (2000) give the results of more sophisticated modelling. Here, the phase space distribution function of the globular cluster and the satellite galaxy population is built and then convolved with the errors to find the probability of the dataset given the model parameters. This is inverted using Bayesian likelihood techniques to give the probability of the enclosed mass given the positions and velocities of the halo globular clusters. Using the combined globular cluster and satellite galaxy sample, they reckoned that the most likely total mass of M31 is $\sim 12_{-6}^{+18} \times 10^{11} M_\odot$. An independent constraint on the mass of M31 within 30 kpc is given by the HI rotation curve. This was measured to distances of ~ 30 kpc along the major axis by Newton & Emerson (1977). Their estimate of the asymptotic circular speed is 230 km s^{-1} . Assuming the circular velocity curve maintains this amplitude out to 100 kpc, then the mass within 100 kpc is $1.2 \times 10^{12} M_\odot$. We conclude that the results are all consistent and support a picture in which M31’s dark halo extends out in an isothermal-like manner to at least 100 kpc.

3.2. Satellite Galaxies

There are 15 probable companion galaxies to M31. Their galactic coordinates, projected position from the center of M31 and line of velocity are listed in Table 3. The observed radial velocities contain contributions from the Galactic rotation and from the relative velocity between the Galaxy and M31. Assuming that the transverse velocity of M31 with respect to the Galaxy is zero, we remove these contributions and list the corrected velocities in the frame of M31 in Table 3.

The number density of M31’s satellite galaxies falls like $r^{-3.5}$ (see e.g., Evans & Wilkinson 2000). Notice that the projected positions of many of the objects lies well beyond the régime

in which the M31 halo is expected to be isothermal. Rather, the underlying gravitational potential is probably dominated by the monopole component at such huge distances. This suggests that it is appropriate to apply the tracer mass estimate with $\alpha \approx 1$ and $\gamma \approx 3.5$ to the satellite galaxy dataset. This gives the mass of M31 as $\sim 1.1 \times 10^{12} M_{\odot}$. This is in good agreement with the more sophisticated modelling in Evans et al. (2000), who claimed that the total mass is $7 - 10 \times 10^{11} M_{\odot}$ from the same dataset. In fact, it is in excellent accord with still earlier work by Bahcall & Tremaine (1981), who also found a mass of $\sim 1.0 \times 10^{12} M_{\odot}$ from just five companions (M32, M33, NGC 147, NGC 185 and NGC 205). Despite the seeming agreement, the uncertainty in the mass is at least a factor of 3. For example, if instead we choose $\alpha \approx 0.5$ (suitable for a halo with a rotation curve slowly falling like $\propto r^{-0.25}$), then the mass of M31 as deduced from the tracer estimator more than triples to $\sim 3.8 \times 10^{12} M_{\odot}$.

An assumption underlying the tracer mass estimator (as well as the projected and virial estimators) is that of a steady state equilibrium. This is reasonable enough for globular cluster and PNe datasets, but probably not for satellite galaxies. The dSph and dIrr companions of M31 may well be falling in for the first time, in which case the assumption of a steady state is probably not a valid description of the dynamics. It would be valuable to calibrate the importance of the effects of disequilibrium against high resolution N-body simulations of the Local Group.

4. Conclusions

The main accomplishment of this paper is the introduction of the *tracer mass estimator*. This is a new and simple way of estimating the enclosed mass from the radial velocities and projected positions of a set of objects. It is tailored for the case of tracer populations such as globular clusters and halo stars whose number density falls off like a power-law with distance (at least within the range covered by the survey). The estimator works by averaging the quantity $(\text{constant}) \times (\text{projected distance}) \times (\text{radial velocity})^2 / G$ over the sample. The value of the constant is straightforward to calculate. It depends on the radial fall-off of the tracers, the inner and outer radii marking the range of the sample, the velocity anisotropy of the population and the underlying gravitational potential. In the absence of further information, we recommend assuming isotropy and isothermality for estimating galaxy masses, at least in the case of globular cluster and planetary nebulae (PNe) datasets. The inner and outer radii can usually be inferred from the sample itself, sometimes using additional astrophysical evidence.

We have applied the tracer mass estimator to the globular cluster and satellite galaxy

Table 3: Data on the companion galaxies of M31 taken from Grebel (2000) and Evans et al. (2000). Listed are Galactic coordinates (ℓ, b), the projected distance from the center of M31 R in kpc, corrected line of sight velocities v_{los} (adjusted for the solar motion within the Galaxy and the radial motion towards M31) and object type. (Note: the coordinates for the Cas dSph given in Table 1 of Evans et al. (2000) are incorrect).

Name	ℓ	b	R	v_{los}	Type
M31	121.2	-21.6	–	–	SbI-II
M32	121.1	-22.0	5	+95	E2
NGC 205	120.7	-21.1	8	+58	dSph
NGC 147	119.8	-14.3	100	+118	dSph/dE5
NGC 185	120.8	-14.5	95	+107	dSph/dE3
M33	133.6	-31.5	198	+72	ScII-III
IC 10	119.0	-3.3	243	-29	dIrr
LGS3	126.8	-40.9	262	-38	dIrr/dSph
Pegasus	94.8	-43.5	397	+86	dIrr/dSph
IC 1613	129.7	-60.6	489	-58	IrrV
And I	121.7	-24.9	44	-85	dSph
And II	128.9	-29.2	138	+82	dSph
And III	119.3	-26.2	67	-58	dSph
And V	126.2	-15.1	07	-107	dSph
And VI	106.0	-36.3	260	-65	dSph
Cas dSph	109.5	-9.9	215	+23	dSph

datasets of the Andromeda galaxy (M31). The estimates suggest a picture in which M31’s dark halo is isothermal out to at least ~ 100 kpc and has a mass of $\sim 1.2 \times 10^{12} M_{\odot}$. These estimates are in good agreement with the results of more sophisticated modelling. The advantage of the tracer mass estimator is that it is so much quicker to apply and requires much less effort. It should be used in preference to the projected mass estimator for populations in the outer parts of galaxies. One of the fundamental assumptions of the projected mass estimator (at least in the form which it is usually encountered) is that the population shadows the overall mass density. This assumption breaks down for populations in the outer parts of galaxies. We envisage the tracer mass estimator as being particularly useful for early-type galaxies for which there is no gas rotation curve and so mass estimates

almost always derive from dynamical modelling of tracer populations.

NWE thanks the Royal Society and MIW thanks PPARC for financial support. We are grateful to the (anonymous) referee for providing a helpful report.

REFERENCES

- Aurière M. et al. 2001, *ApJ*, 553, L137
- Bahcall J., Tremaine S. 1981, *ApJ*, 244, 805
- Binney J. 1981, In “Structure and Evolution of Normal Galaxies”, Eds. D. Lynden-Bell, S.M. Fall, (Cambridge University Press, Cambridge) p. 55
- Evans N.W., Häfner R.M., de Zeeuw P.T., 1997, *MNRAS*, 286, 315
- Evans N.W., Wilkinson M.I., 2000, *MNRAS*, 316, 929
- Evans N.W., Wilkinson M.I., Guhathakurta P., Grebel E.K., Vogt S.S. 2000, *ApJ*, 540, L9
- Grebel E.K. 2000, in 33rd ESLAB Symp., Star Formation from the Small to the Large Scale, ed. F. Favata, A.A. Kaas, C. Wilson (Noordwijk: ESA), p. 87
- Halliday C., Carter D., Jackson Z., Bridges T.J., Evans N.W., Wilkinson M.I. 2002. In “IAU Symposium 209: Planetary Nebulae: Their Evolution and Role in the Universe”, Eds. M. Dopita et al., ASP Conf Series, in press.
- Heisler J., Tremaine S., Bahcall J.N. 1985, *ApJ*, 298, 8
- Hodge P. 1992, *The Andromeda Galaxy* (Kluwer, Dordrecht)
- Huchra J.P., Brodie J.P., Kent S.M. 1991, *ApJ*, 370, 495
- Méndez R.H., Riffeser A., Kudritzki R.-P., Matthias M., Freeman K.C., Arnaboldi M., Capaccioli M., Gerhard O.E. 2001, *ApJ*, 563, 135
- Newton K., Emerson D.T. 1977, *MNRAS*, 181, 573
- Paulin-Henriksson S. et al. 2002, *A&A*, in press
- Perrett K.M., Bridges T.J., Hanes D.A., Irwin M.J., Brodie J.P., Carter D., Huchra J.P., Watson F.G. 2002, *AJ*, 123, 2490

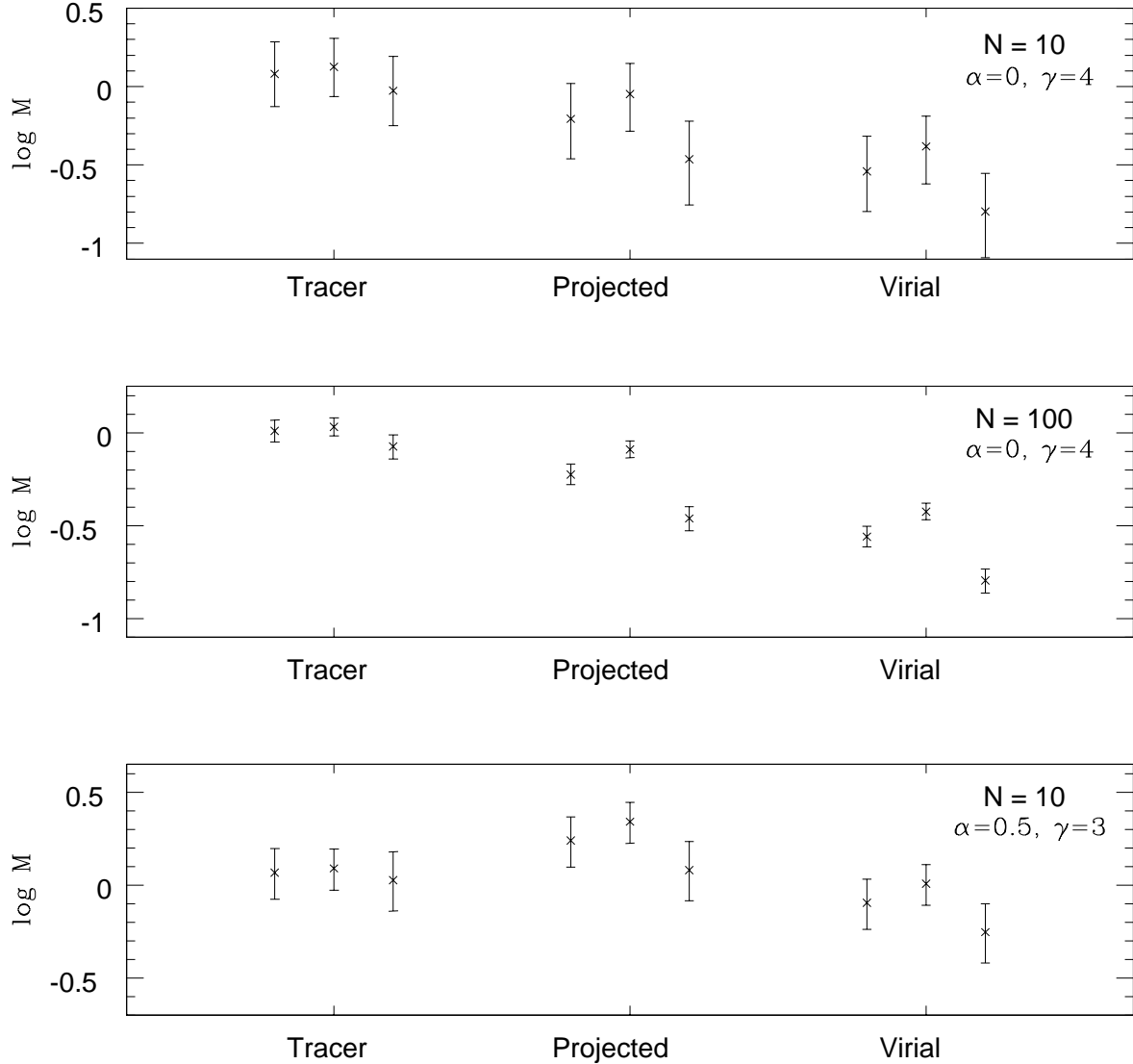


Fig. 1.— Medians and upper and lower quartiles for the mass estimates of 10000 tracer samples constructed from realisations of exact scale-free models. Upper Panel: The tracer population has a number density falling like r^{-4} in an isothermal potential. The data is gathered between $R_{\text{out}} = 10R_{\text{in}}$. From left to right, the models are: (i) 10 objects drawn from an isotropic velocity distribution, (ii) 10 objects drawn with $\sigma_t : \sigma_r = 2 : 1$, and (iii) 10 objects with $\sigma_t : \sigma_r = 1 : 2$. For anisotropic populations, knowledge of the anisotropy β is assumed and the tracer mass estimator in the general form (16) is used. Middle Panel: As the Upper Panel, but the number of objects is now 100. Lower Panel: As the Upper Panel, but the tracer population has a number density falling like r^{-3} in a potential with a falling rotation curve $\psi \propto r^{-1/2}$.

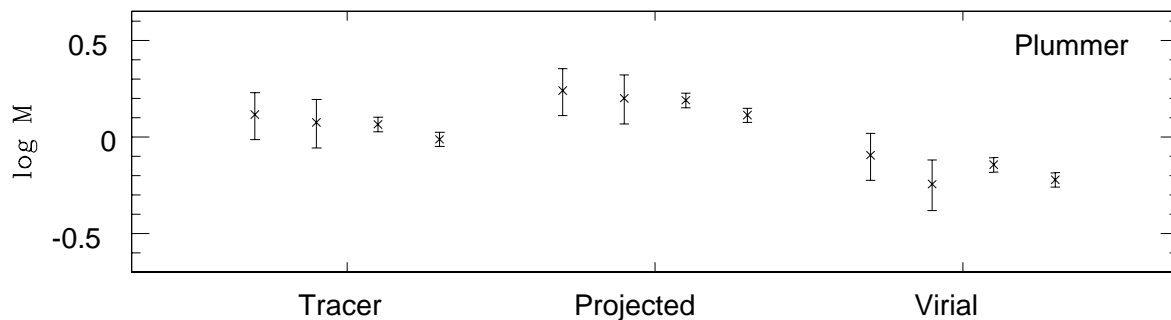


Fig. 2.— Medians and upper and lower quartiles for the mass estimates of 10000 tracer samples constructed from realisations of exact Plummer models with core radius b . The self-consistent population has a number density falling like r^{-5} in a potential falling like r^{-1} at large radii. Again, the performance of the tracer, projected and virial mass estimators is compared. From left to right, the models are: (i) 10 objects gathered between $R_{\text{in}} = 10b$ and $R_{\text{out}} = 100b$, (ii) 10 objects between $R_{\text{in}} = b$ and $R_{\text{out}} = 100b$, (iii) the same as (i) but with $N = 100$, and (iv) the same as (ii) but with $N = 100$.

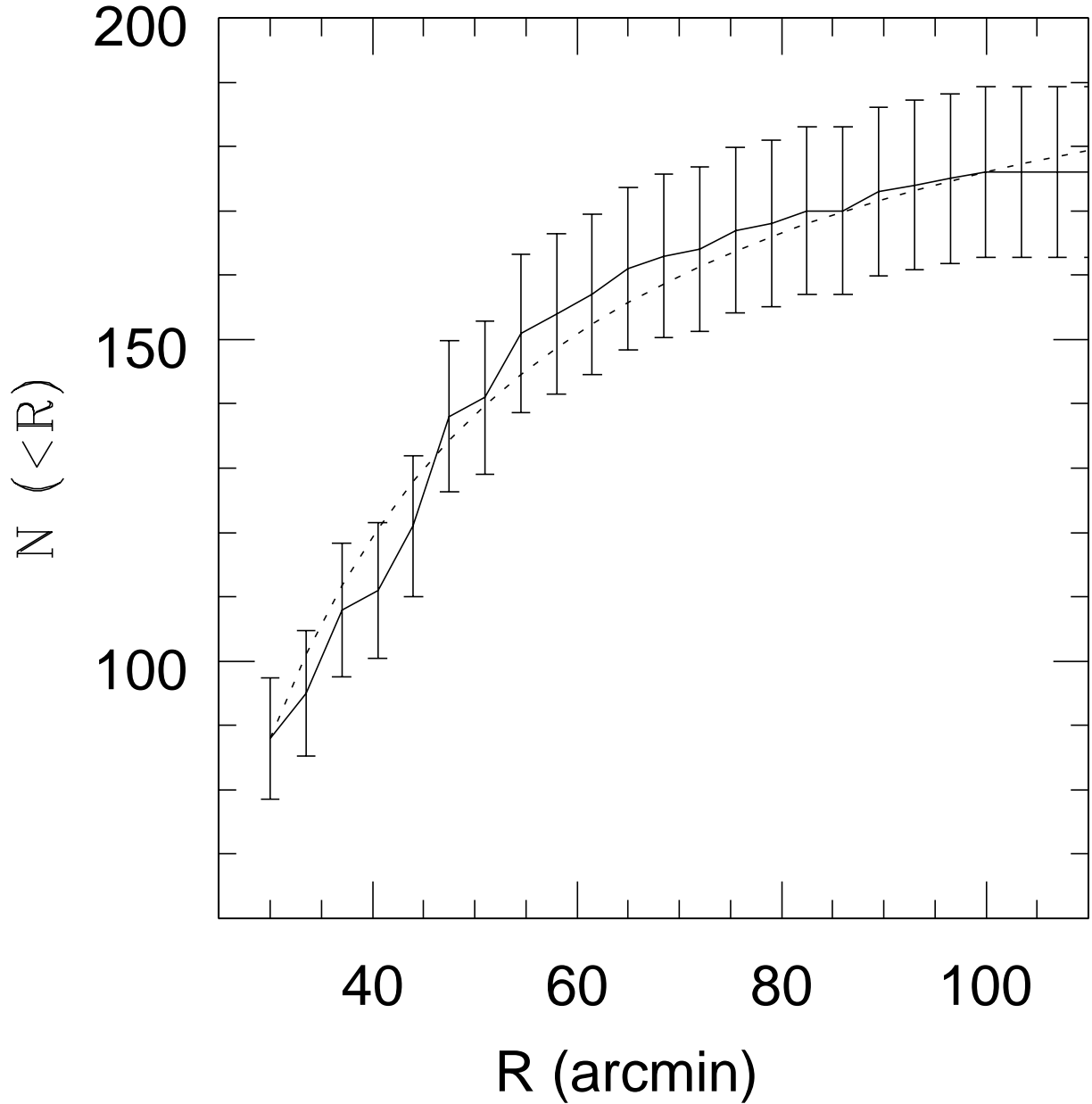


Fig. 3.— Cumulative number N of M31 halo globular clusters versus projected radius R (in arcmin). The dotted line shows the profile expected for a population with three dimensional density distribution $\rho \sim r^{-4}$ between $30'$ and $100'$.

Sellwood J.A. 2000, ApJ, 540, L1

Smart W.M., 1938, Stellar Dynamics, Cambridge University Press, Cambridge

Wilkinson M.I., Evans N.W. 1999, MNRAS, 310, 645

Wilkinson M.I., Kleyna J.T., Evans N.W., Gilmore G., 2002, In “The Mass of Galaxies at Low and High Redshift”, Eds. R. Bender, A. Renzini, (Springer-Verlag: New York), in press.

Zwicky F. 1933, Helv. Phys. Acta., 6, 110